

## Charge Recombination in Zinc Oxide-Based Dye-Sensitized Solar Cell: A Mini Review

Kaiswariah Magiswaran<sup>1,2</sup>, Mohd Natashah Norizan<sup>1,2,a\*</sup>, Ili Salwani Mohamad<sup>1,2</sup>, Norsuria Mahmed<sup>1,3,b\*</sup>, Siti Norhafizah Idris<sup>1,2</sup> and Sharizal Ahmad Sobri<sup>1,4</sup>.

<sup>1</sup>Geopolymer & Green Technology, Centre of Excellence (CEGeoGTech), Universiti Malaysia Perlis (UniMAP), Perlis, Malaysia.

<sup>2</sup>Faculty of Electronic Engineering Technology, Universiti Malaysia Perlis (UniMAP), Perlis, Malaysia.

<sup>3</sup>Faculty of Chemical Engineering Technology, Universiti Malaysia Perlis (UniMAP), Perlis, Malaysia.

<sup>4</sup>Advanced Material Research Cluster, Faculty of Bioengineering and Technology, Universiti Malaysia Kelantan, Jeli Campus, 17600 Jeli, Kelantan, Malaysia.

### ABSTRACT

*Dye-sensitized solar cell (DSSC) has been studied widely due to its efficiency and the simplicity of manufacturing technology. Much research has been performed to improve the photovoltaic output parameters in DSSC by modifying the photoanode layers. The efforts to investigate DSSC mainly focus on how to increase light absorption, speed electron transport in circuits, and reduce charge recombination. This review discusses the process of charge recombination and the paths of occurrence in a DSSC. Recombination occurs when the electrons in the conduction band fall into the valance band holes and is considered an unnecessary process in DSSC. Due to the recombination process, the photocurrent and the photovoltage are reduced, leading to lower power conversion efficiency. Hence, the ways to overcome the charge recombination process were also discussed.*

**Keywords:** Charge recombination, dye-sensitized solar cell (DSSC), doped ZnO photoanode.

### 1. INTRODUCTION

Photovoltaic panels are one of the most promising technologies ever developed in the field of renewable energy [1]. It was due to their ability to absorb the sun's rays and turn solar energy into electricity [2]. Solar energy (photons) is captured and converted into electrical energy in DSSCs [3] using the photovoltaic effect [4]. DSSCs are made up of a conductively coated glass substrate (TCO), a photoanode (working electrode), a counter electrode, electrolyte, and dye [5-6]. The mesoporous film used in DSSC productions usually has a thicknesses range of 10 -12  $\mu\text{m}$  [7], 20 nm diameter particles [8], and a porosity of 50 %. These features will absorb incident light [9], resulting in an 11.2 % power conversion efficiency [10].

The ease of manufacture, low-cost materials, and benefits related to clarity makes DSSC the most promising photovoltaic device available [11]. However, the poor photo-electric conversion efficiency and stability of DSSCs pose a significant barrier to their commercialization [6]. According to Shockley Queisser limit estimation for single-junction cells, the overall theoretical conversion energy efficiency for DSSC has been calculated to be 32 % [12-13], but the highest efficiency recorded so far is only 13% [14]. The charge recombination process is one of the main reasons that cause the efficiency of a DSSC to decrease. In order to improve the efficiency of the DSSC, researchers have made extensive efforts in understanding the parameters that affect its performance. In addition, attempts have been made to improve the photoanode quality through surface modifications of the semiconductor materials [4, 14-15].

---

<sup>a\*</sup>mohdnatashah@unimap.edu.my, <sup>b\*</sup>norsuria@unimap.edu.my

In this review, the charge recombination of electron-hole pairs at the interfaces of the DSSC and the surface modifications are done on the photoanodes to improve the efficiency of the cell will be discussed.

## 2. COMPONENTS AND WORKING PRINCIPLES OF A DSSC

The essential components of DSSCs primarily consist of transparent conducting oxide (TCO) film-coated glass substrate, dye, photoanode, electrolytes, and counter electrode [5]. A typical photoanode material consists of dye molecules-adsorbed semiconductor oxide material coated on TCO substrate, which acts as a working electrode in DSSCs [17]. The most widely used semiconductor materials are titanium dioxide ( $\text{TiO}_2$ ) [4, 14]. Other than  $\text{TiO}_2$ , zinc oxide ( $\text{ZnO}$ ) [10, 18] and tin oxide ( $\text{SnO}_2$ ) [19] were also used as photoanode scaffold material in DSSC. Among these materials, the  $\text{ZnO}$  semiconductor material has recently caught the eyes of researchers due to its similar properties to  $\text{TiO}_2$  and is considered the best replacement for  $\text{TiO}_2$  material [10, 20]. Table 1 shows the differences in the properties of both  $\text{TiO}_2$  and  $\text{ZnO}$  material.

**Table 1** Comparison of physical properties of  $\text{ZnO}$  and  $\text{TiO}_2$ .

Properties	$\text{TiO}_2$	$\text{ZnO}$	Ref
<b>Band gap</b>	3.2eV	3.3eV	[14, 17, 18]
<b>Cost</b>	Abundant, cost effective	Lower in cost	[6, 11]
<b>Surface area</b>	High surface area	Larger surface area	[20]
<b>Electron Mobility</b>	Limited electron mobility 0.1-4.1 $\text{cm}^2\text{V}^{-1}\text{s}^{-1}$	Higher electron mobility 200-300 $\text{cm}^2\text{V}^{-1}\text{s}^{-1}$	[10, 20, 21]
<b>Charge recombination</b>	Charge recombination occurs due to the short electron-hole recombination time	Able to eliminate charge recombination due to the higher electron mobility and fast electron diffusion	[22-24]

$\text{ZnO}$  is a semiconductor material from group II-VI compound [20]. It is an n-type semiconductor with a hexagonal wurtzite structure and a direct bandgap of 3.37 eV at room temperature [46, 47]. It shows excellent electronic properties with the ease of crystallization [10], anisotropic growth, and more extended electron mobility (200-300  $\text{cm}^2\text{V}^{-1}\text{s}^{-1}$ ) [28].  $\text{ZnO}$  nanostructures proved to provide a remarkable enhancement in the efficiency of the DSSC due to their effective light-harvesting efficiency [22] and large surface area for the adsorption of dye [29]. A DSSC with  $\text{ZnO}$  can reduce the charge recombination reactions compared to a DSSC with  $\text{TiO}_2$  [10, 23].

In  $\text{ZnO}$ -based DSSC structure, fluorine-doped tin oxide (FTO) is considered the most suitable TCO glass as the substrate for the photoanode and counter electrode [30]. Electrolyte is one of the most significant factors affecting the performance of DSSCs [5, 18], where it diffuses within the oxide layer, allowing for internal electric ion conductivity [30]. Iodide/triiodide ( $\text{I}^-/\text{I}_3^-$ ) is a widely used electrolyte in the DSSC [31]. Counter electrode, on the other hand, should have high electrocatalytic activity for redox reactions involving iodide and triiodide [32]. Apart from that, the counter electrode should be robust [33], low-resistance [34], and transparent. Due to its ability to catalyze the triiodide ions in the electrolyte, the platinum (Pt) counter electrode [20, 22] is reported to be the most suitable and commonly used counter electrode in DSSCs. In a DSSC, the dye serves as a molecular pump [30] and absorbs a range of visible light [24]. The most reliable dye is N719 [36], which is used as a baseline for the DSSC [25-26]. The DSSC structure arrangements and working theory [5, 16] are shown in Figure 1.

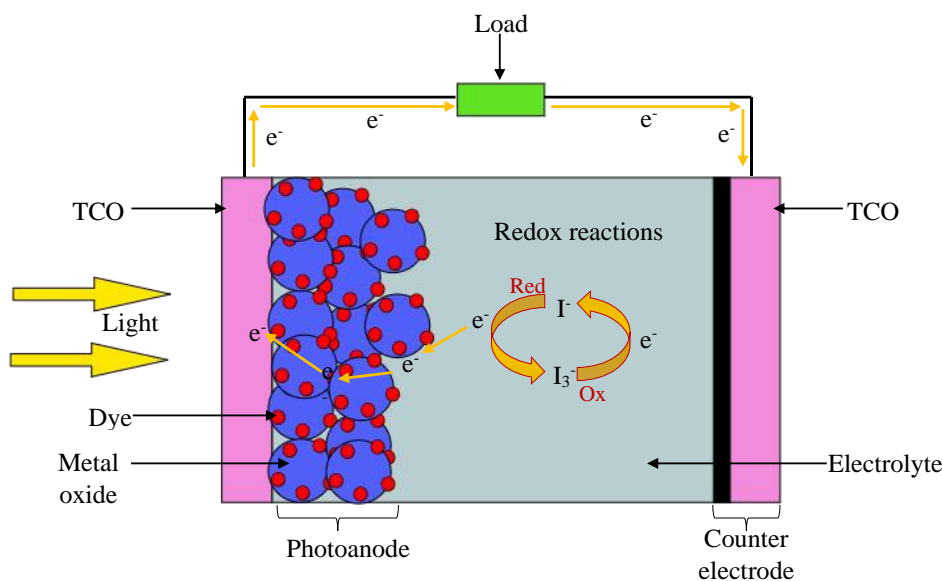


**Figure 1.** Components and working principle of a DSSC [5]

The incident photons are absorbed by the dye molecules attached to the semiconductor oxide surface [31], which become excited. In the excited state, electron-hole pair is generated, and the dye molecules deliver electrons into the conduction band of semiconductor oxide and become oxidized [5]. The injected electrons pass through the semiconductor layer into the load before arriving at the counter electrode [6]. After that, the electrons diffuse through the electrolyte and pass electrons to the oxidized dye [35]. Simultaneously, the iodide molecules in the electrolyte will oxidize to triiodide [17]. Finally, these oxidized molecules will make their way to the counter electrode [9], which will be regenerated by external electrons [38].

### 3. CHARGE RECOMBINATION PROCESS IN A DSSC

Semiconductor oxides contain conduction and valence bands. The conduction band contains free electrons, whereas the valence band contains holes [39]. The generation and recombination occur when the electron transitions from the valence band to the conduction band and vice-versa [40]. A hole is a vacancy created by the electrons [30-31]. When the free electron and hole are merged, it is known as carrier recombination [20, 32]. A recombination reaction in a semiconductor material is defined as when the electrons in the conduction band fall into holes in the valence band. Then, free electrons and holes disappear or are eliminated [9, 14, 33-34]. Thus, the hole-electron pairs disappear as a result of recombination. The same concept is applied in DSSC. However, the recombination process of the electron is considered unnecessary in DSSC [35-37]. Due to the recombination process, the photocurrent and the photovoltage are reduced, leading to lower power conversion efficiency [35, 38-39].

#### 3.1 The paths of charge recombination

There are several interfaces in a DSSC cell where the charge recombination can take place. When the dye ( $D/D^*$ ) receives photons, it gets excited and moves from the ground state to the excited state [51]. Then, the electrons will pass through the semiconductor oxide through the electrolyte ( $R/R^*$ ). However, before the electrons get to move into the semiconductor oxide, it falls back to the ground state of the dye and recombines with the hole [41-42], as shown in route 1 [51]. This process takes place at the dye/electrolyte/semiconductor oxide interface [41-42]. Route 2 is when the electron passes through the semiconductor oxide successfully and moves into the TCO.

Nevertheless, due to the thick layer of the semiconductor materials (mesoporous layer), the electron recombines with electrolyte solution [40, 43]. This reaction occurs at the semiconductor oxide/electrolyte interfaces. Route 3 happens when the electrons from the substrate (TCO) recombines with the redox electrolyte [40-41]. Figure 2 below shows the detailed charge recombination process and the electron movements through the DSSC [40-43].

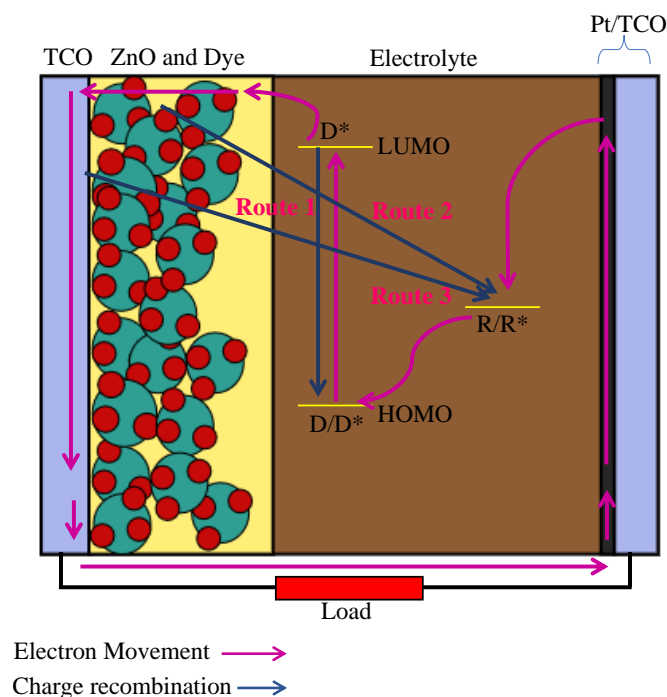


**Figure 2.** Routes of charge recombination in DSSC [40–43]

#### 4. DOPED ZNO PHOTOANODE TO ELIMINATE THE CHARGE RECOMBINATION PROCESS

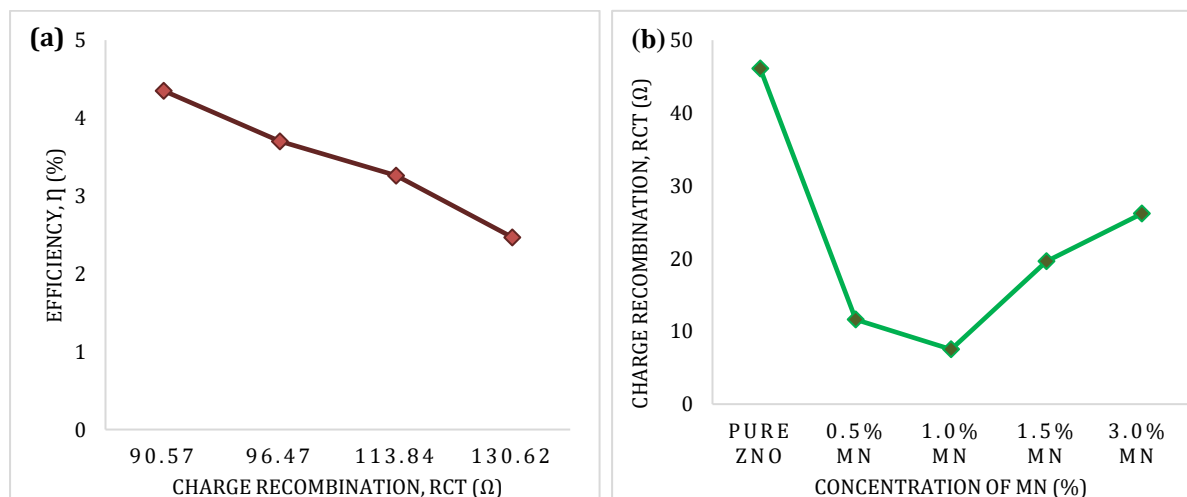
Doping represents a valuable approach to tune various ZnO properties. Doping involves inserting a specific ion into a crystal lattice not initially present in the starting material [55]. It can be advantageous to modulate the energy bandgap, directly affecting the ZnO photocatalytic properties [56]. The doping of the ZnO material plays a dual role in the DSSC performance, including enhancing the absorption coefficient of the dye [38, 44] and optical absorption due to surface plasmonic resonance [14, 39]. Moreover, they act as an electron sink for photo-induced charge carriers [16], improve the interfacial charge transfer process [49], and minimize the charge recombination process, thereby enhancing the electron transfer process in a DSSC [22, 35].

Table 2 shows the different types of ZnO doped photoanodes. When the plasmonic nanoparticles (silver and gold) are doped on the metal oxide nanoparticles, a Schottky barrier can be formed between the plasmonic nanoparticles and the semiconductor [14, 39]. When an electron in the lowest unoccupied molecular orbital (LUMO) of the dye tunnels to the conduction band and the semiconductor via the plasmonic nanoparticles, it is unlikely to go back to either the dye or the electrolyte due to the presence of the Schottky barrier [16]. While, the rare earth oxide layer such as europium ( $\text{Eu}_2\text{O}_3$ ) forms an energy barrier on nanoparticles, which effectively inhibits the surface charge recombination and improves the energy conversion efficiency of the DSSC [58]. It can be seen that the doping elements in the ZnO photoanodes affecting the efficiency of the cell by increasing their photocurrent and photovoltage. The higher efficiency of the doped ZnO photoanode proves that charge recombination is reduced.

**Table 2** Different types of photoanodes and their efficiency

Photoanode	$J_{sc}$ (mA/cm <sup>2</sup> )	$V_{oc}$ (V)	$\eta$ (%)	Ref
Pure ZnO	5.61	0.55	1.45	
Mn doped ZnO	11.56	0.63	4.20	[59]
ZnO	5.50	0.81	2.62	
Ag-ZnO	6.25	0.80	3.51	[28]
ZnO	6.96	0.69	2.47	
Au doped ZnO	9.97	0.71	4.35	[60]
ZnO	1.34	0.60	0.44	
Eu <sub>2</sub> O <sub>3</sub> doped ZnO	4.51	0.70	1.45	[58]
ZnO	2.70	0.57	0.99	
Nb <sub>2</sub> O <sub>5</sub> doped ZnO	3.99	0.70	2.39	[61]

Liu et al. developed gold doped ZnO nanoparticles with an efficiency of 8.91%. They stated that the charge recombination process decreases when the amount of Au nanoparticles increases. The Au/ZnO NPs based DSSC, but the Schottky barrier between the metal/semiconductor interface functions as an electron-hole separation center. They suggested that the optimum amount of Au need to be added to obtain optimal charge separation condition [50]. Figure 3(b) [59] shows that the charge recombination highly depends on the concentration of the doping element. The charge recombination,  $R_{ct}$ , reaches the lowest when ZnO is doped with an optimum concentration of Mn [59]. The ZnO/Nb<sub>2</sub>O<sub>5</sub> bilayer photoanode prepared by Niyamat et al. increased the electron lifetime and decreased the magnitude of the electron recombination compared to the photoanode without the Nb<sub>2</sub>O<sub>5</sub> layer. The bilayer ZnO/Nb<sub>2</sub>O<sub>5</sub> significantly enhanced recombination resistance and increased efficiency by about 6% more than the ZnO-based DSSC [62].



**Figure 3.** (a) The charge recombination vs. the efficiency of the DSSC (b) The concentration of doped particles vs. the charge recombination [59]

Aneesiya et al. developed strontium-doped ZnO nanorods with different concentrations to overcome the charge recombination process in the ZnO-based DSSCs. The charge transfer resistance in the doped ZnO-based DSSC was lesser than the undoped ZnO-based DSSC. This ZnO/N<sub>3</sub>/electrolyte interface reduced transport resistance at Pt-electrode in the Sr doped ZnO DSSC. The electron-hole recombination was reduced, and efficient charge transportation in doped ZnO-based DSSC resulted in an increased short-circuit current density and photovoltaic conversion efficiency. Figure 3(a) shows that the efficiency of the DSSC cell is higher when the charge recombination of the cell is the lowest. Erdi Akman developed compact layers of europium

and manganese-doped ZnO particles to enhance the electron transport mechanism of the ZnO photoanode [59]. The manganese-doped ZnO with europium compact layer was able to show a lower charge transport resistance than the pure DSSC, which implies an improvement in the electron transport and the performance of DSSC [59].

## 5. RECOMMENDATION

Recombination is one of the most critical factors affecting the electron transport in DSSC, and the improvement of the performance of DSSC can be achieved when the recombination is reduced. From recent researches, the plasmonic particles (gold and silver) doped ZnO based DSSC has a better standing in eliminating the charge recombination process. However, there are not enough studies showing the exact mechanisms of the recombination reaction in a DSSC. Hence, to improve the efficiency and performance of a DSSC, the charge recombination process should be studied more widely, and it is essential to come up with strategies to hinder the charge recombination process in ZnO-based DSSCs.

## ACKNOWLEDGEMENT

The author would like to acknowledge the Fundamental Research Grant Scheme (FRGS) support under the grant number FRGS/1/2020/TK0/UNIMAP/02/35 from the Ministry of Higher Education Malaysia and Universiti Malaysia Perlis.

## REFERENCES

- [1] P. G. V. Sampaio, M. O. A. González, *Renew. Sustain. Energy Rev.*, vol. **74**, (2016), pp. 590-601.
- [2] S. Nair, S. B. Patel, and J. V. Gohel, *Mater. Today Energy*, vol. **17**, (2020) p. 100449.
- [3] V. Sugathan, E. John, and K. Sudhakar, *Renew. Sustain. Energy Rev.*, vol. **52**, (2015) pp. 54-64.
- [4] J. Gong, K. Sumathy, Q. Qiao, and Z. Zhou, *Renew. Sustain. Energy Rev.*, vol. **68**, (2017) pp. 234-246.
- [5] S. N. Karthick, K. V. Hemalatha, S. K. Balasingam, F. Manik Clinton, S. Akshaya, and H. J. Kim, *Interfacial Eng. Funct. Mater. Dye. Sol. Cells*, (2019) pp. 1-16.
- [6] H. Aliah et al., "Dye Sensitized Solar Cells (DSSC) Performance Reviewed from the Composition of Titanium Dioxide (TiO<sub>2</sub>)/Zinc Oxide (ZnO)," in *IOP Conf. Ser. Mater. Sci. Eng.*, vol. **288**, no. 1 (2018).
- [7] M. S. Wu and R. S. Yang, *J. Alloys Compd.*, vol. **740**, (2018) pp. 695-702.
- [8] G. Zamiri and S. Bagheri, *J. Colloid Interface Sci.*, vol. **511**, (2018) pp. 318-324.
- [9] A. Dennyson Savariraj, R. V. V. Mangalaraja, A. D. Savariraj, and R. V. V. Mangalaraja, *Interfacial Eng. Funct. Mater. Dye. Sol. Cells*, (2019) pp. 17-33.
- [10] R. Vittal and K.-C. Ho, *Renew. Sustain. Energy Rev.*, vol. **70**, (2017) pp. 920-935.
- [11] N. Jamalullail, I. S. Mohamad, M. N. Norizan, N. Mahmed, and B. N. Taib, "Recent improvements on TiO<sub>2</sub> and ZnO nanostructure photoanode for dye sensitized solar cells: A brief review," in *EPJ Web Conf.*, vol. **162**, (2017) pp. 1-5.
- [12] A. K. Rajan and L. Cindrella, *Superlattices Microstruct.*, vol. **128**, no. September 2018, (2019) pp. 14-22.
- [13] M. Shakeel Ahmad, A. K. Pandey, and N. Abd Rahim, " *Renew. Sustain. Energy Rev.*, vol. **77** (2017) pp. 89-108.
- [14] M. E. Yeoh and K. Y. Chan, *Int. J. Energy Res.*, vol. **41**, (2017) pp. 2446-2467.
- [15] P. Zhao et al., *Electrochim. Acta*, vol. **176**, (2015) pp. 845-852.
- [16] S. P. Lim, *Interfacial Eng. Funct. Mater. Dye. Sol. Cells*, (2019) pp. 193-21.

- [17] S. R.S. Shelke, *Int. J. Renew. Energy Resour.* (formerly *Int. J. Renew. Energy Res.*, vol. **Volume 3**, no. Issue 2, (2014) pp. 54–61.
- [18] A. Omar and H. Abdullah, *Renew. Sustain. Energy Rev.*, vol. **31**, (2014) pp. 149–157.
- [19] Q. Wali, A. Fakhruddin, and R. Jose, *J. Power Sources*, vol. **293**, (2015) pp. 1039–105 .
- [20] J. A. Anta, E. Guillén, and R. Tena-Zaera, *J. Phys. Chem. C*, vol. **116**, no. 21, (2012) pp. 11413–11425.
- [21] V. Parihar, M. Raja, and R. Paulose, *Rev. Adv. Mater. Sci.*, vol. **53**, no. 2, (2018) pp. 119–130.
- [22] J. J. Mock et al., *Appl. Phys. Lett.*, vol. **86**, no. 3, (2012) pp. 4087–4108.
- [23] A. R. A. Rashid, N. A. Kamarudin, I. S. Mohamad, and M. N. Norizan, *Int. J. Nanoelectron. Mater.*, vol. **11**, (2019) pp. 187–194.
- [24] A. Dennyson Savariraj and R. V. Mangalaraja, *Interfacial Eng. Funct. Mater. Dye. Sol. Cells*, (2019) pp. 17–33 .
- [25] E. Kouhestanian, M. Ranjbar, S. A. Mozaffari, and H. Salaramoli, *Prog. Color Color. Coat*, vol. **14**, (2020) pp. 101–112.
- [26] S. G. Kumar and K. S. R. K. Rao, *Appl. Surf. Sci.*, vol. **391**, (2017) pp. 124–148.
- [27] I. S. Mohamad, M. N. Norizan, M. K. F. M. Hanifah, I. A. M. Amin, and M. M. Shahimin, "Fabrication and characterization of ZnO:In thin film as photoanode for DSSC using natural fruit dyes," in *AIP Conf. Proc.*, vol. **1660** (2015).
- [28] V. S. S. Manikandan, A. K. K. Palai, S. Mohanty, and S. K. Nayak, *Ceram. Int.*, vol. **44**, no. 17, (2018) pp. 21314–21322.
- [29] E. Kouhestanian, M. Ranjbar, S. A. Mozaffari, and H. Salaramoli, *Prog. Color. Color. Coatings*, vol. **14**, no. 2, (2021) pp. 101–112.
- [30] K. Sharma, V. Sharma, and S. S. Sharma, *Nanoscale Res. Lett.*, vol. **13** (2018).
- [31] N. T. R. N. Kumara, A. Lim, C. M. Lim, M. I. Petra, and P. Ekanayake, *Renew. Sustain. Energy Rev.*, vol. **78**, (2017) pp. 301–317.
- [32] M. Berginc, U. Opara Krašovec, M. Jankovec, and M. Topič, *Sol. Energy Mater. Sol. Cells*, vol. **91**, no. 9, (2007) pp. 821–828
- [33] J. Wu, Z. Tang, Y. Huang, M. Huang, H. Yu, and J. Lin, *J. Power Sources*, vol. **257**, (2014) pp. 84–89.
- [34] P. Balraju, P. Suresh, M. Kumar, M. S. Roy, and G. D. Sharma, *J. Photochem. Photobiol. A Chem.*, vol. **206**, no. 1, (2009)pp. 53–63.
- [35] D. Kishore Kumar et al., *Mater. Sci. Energy Technol.*, vol. **3**, (2020)pp. 472–48.
- [36] L. N. Dang Quang, A. K. Kaliyamurthy, and N. H. Hao, *Opt. Mater. (Amst)*, vol. **111**, no. September, (2021)p. 110589.
- [37] O. Wiranwetchayan, W. Promnopas, K. Hongstith, S. Choopun, P. Singjai, and S. Thongtem, *Res. Chem. Intermed.*, vol. **42**, no. 4, (2016) pp. 3655–367.
- [38] N. Prabavathy, S. Shalini, R. Balasundaraprabhu, D. Velauthapillai, S. Prasanna, and N. Muthukumarasamy, *Int. J. Energy Res.*, vol. **41**, no. 10, (2017) pp. 1372–1396.
- [39] G. F. Brown and J. Wu, *Laser Photonics Rev.*, vol. **3**, no. 4, (2009) pp. 394–405.
- [40] S. Nur, A. Zaine, N. M. Mohamed, and M. Khatani, "Nanocrystalline Passivized Conductive and," (2020).
- [41] W. Sharmoukh, S. A. Al Kiey, B. A. Ali, L. Menon, and N. K. Allam, *Sustain. Mater. Technol.*, vol. **26**, (2020) p. e00210.
- [42] S. Sasidharan et al., *New J. Chem.*, vol. **41**, no. 3, (2017) pp. 1007–1016.
- [43] A. Das, R. R. Wary, and R. G. Nair, *Solid State Sci.*, vol. **104**, no. March, (2020) p. 106290.
- [44] F. Babar et al., *Renew. Sustain. Energy Rev.*, vol. **129**, no. April, (2020) p. 109919.
- [45] K. S. Rajni and T. Raguram, *Interfacial Eng. Funct. Mater. Dye. Sol. Cells*, (2019) pp. 139–162.
- [46] W. Li et al., *Mater. Lett.*, vol. **243**, (2019) pp. 108–111.
- [47] Z. D. Mahmoudabadi, E. Eslami, and M. Narimisa, *J. Colloid Interface Sci.*, vol. **529**, (2018) pp. 538–546.
- [48] E. Kouhestanian, S. A. Mozaffari, M. Ranjbar, and H. S. Amoli, *Org. Electron.*, vol. **86**, (2020) p. 105915.

- [49] E. Kouhestanian et al., *Prog. Color. Color. Coatings*, vol. **14**, no. 2, (2021) pp. 101–112.
- [50] Q. Liu et al., *J. Power Sources*, vol. **380**, no. February, (2018)pp. 142–148 .
- [51] S. Cells and I. Minda, "Photoinduced Charge Dynamics in Indoline-Dye Sensitised Solar Cells," no. (2014).
- [52] E. Palomares, J. N. Clifford, S. A. Haque, T. Lutz, and J. R. Durrant, *Chem. Commun.*, vol. **2**, no. 14, (2002) pp. 1464–1465.
- [53] M. J. Griffith et al., *Chem. Commun.*, vol. **48**, no. 35, (2012) pp. 4145–4162 .
- [54] S. S. K. Raavi and C. Biswas, *Femtosecond Pump-Probe Spectroscopy for Organic Photovoltaic Devices*, no. March 2021.
- [55] H. J. Lee, S. Y. Jeong, C. R. Cho, and C. H. Park, *Appl. Phys. Lett.*, vol. **81**, no. 21, (2002) pp. 4020–4022.
- [56] T. Fukumura, Z. Jin, A. Ohtomo, H. Koinuma, and M. Kawasaki, *Appl. Phys. Lett.*, vol. **75**, no. 21, (1999) pp. 3366–3368.
- [57] L. Lu, R. Li, K. Fan, and T. Peng, *Sol. Energy*, vol. **84**, no. 5, (2010) pp. 844–853.
- [58] M. K. N. K. Verma, "Performance of Eu 2 O 3 coated ZnO nanoparticles-based DSSC," (2013).
- [59] E. Akman, *J. Mol. Liq.*, vol. **317**, (2020) p. 114223.
- [60] M. Saleem et al., *Nanomaterials*, vol. **11**, no. 3, (2021) pp. 1–14.
- [61] G. Arielo, R. Maia, T. L. Valerio, P. Banczek, and P. Rog, vol. **109**, (2020).
- [62] N. I. Beedri, P. K. Baviskar, A. T. Supekar, Inamuddin, S. R. Jadkar, and H. M. Pathan, *Int. J. Mod. Phys. B*, vol. **32**, no. 19, (2018) pp. 1–5.